

Supporting information to

An ATRP-based approach towards water-borne anisotropic polymer-Gibbsite nanocomposites

Olessya P. Loiko,^a Anne B. Spoelstra,^a Alexander M. van Herk,^{a,b} Jan Meuldijk^a and Johan P.A. Heuts*^a

^a Department of Chemical Engineering and Chemistry, Eindhoven University of Technology, PO Box 513, 5600 MB Eindhoven, The Netherlands. E-mail: j.p.a.heuts@tue.nl

^b Institute of Chemical and Engineering Sciences, 1 Pesek Road, Jurong Island 627833, Singapore.

Synthesis and characterisation of anionic random ATRP copolymer

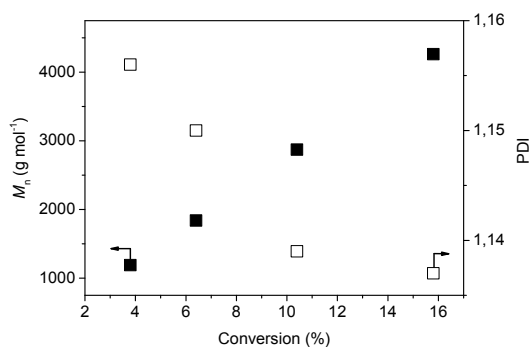


Figure S1. Plot of M_n and PDI vs monomer conversion for BA-co-tBA at [monomer]:[2-bromo-2-methylpropionic acid phenyl ester]= 200:1 in the presence of 10 vol% DMF at 70 °C.

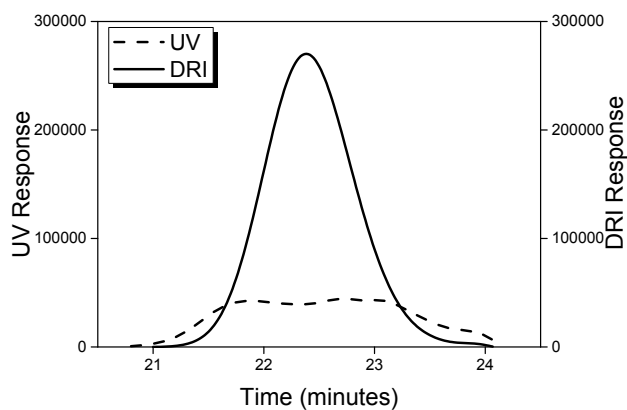


Figure S2. UV and DRI SEC chromatograms of ATRP macroinitiator before hydrolysis

Preparation and characterisation of polymer-Gibbsite latex particles

Effect of $[Cu^{2+}]$ on Gibbsite-ATRP macroinitiator dispersion

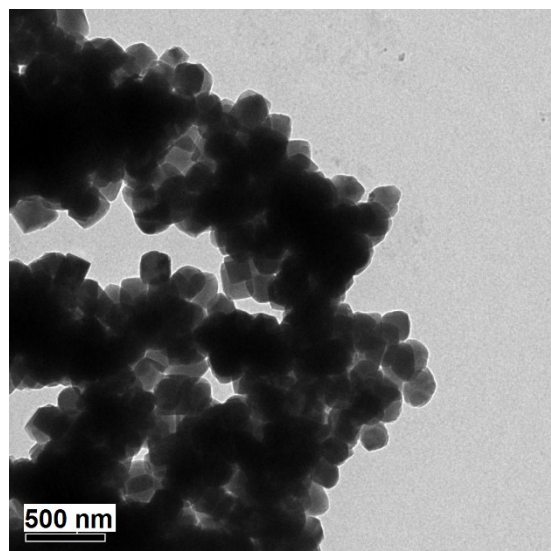


Figure S3. TEM micrograph of colloidal instable Gibbsite platelets after copper (II) catalyst addition.

Effect of monomer feed rate on polymer-Gibbsite latex particles morphology

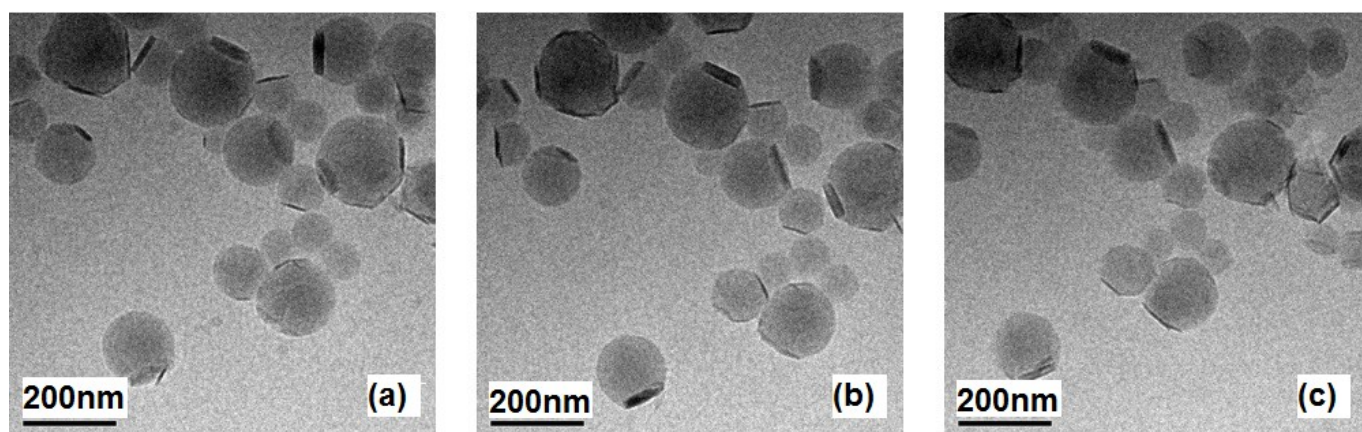


Figure S4. cryo-TEM images of tilt series recorded on polymer-Gibbsite latex particles obtained at the feed rate = 4.6 mg min^{-1} :
(a) tilt $+20^\circ$, (b) tilt 0° , (c) tilt -20° .

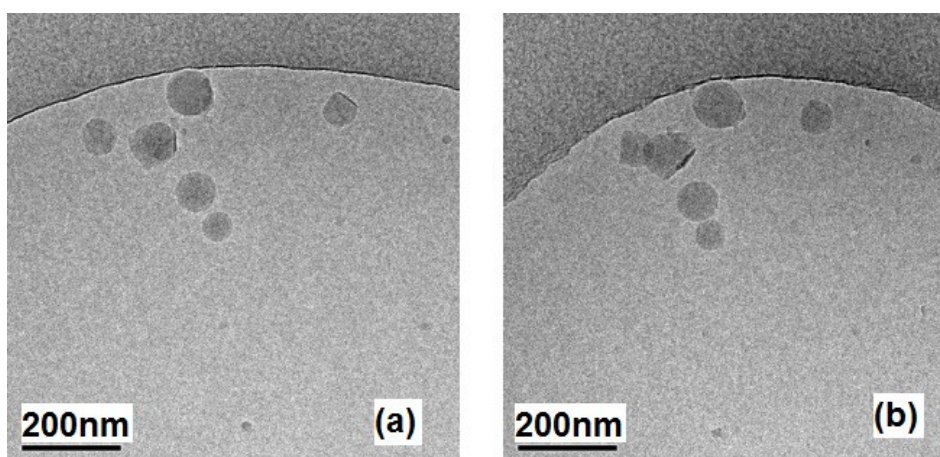


Figure S5. cryo-TEM images of tilt series recorded on polymer-Gibbsite latex particles obtained at the feed rate = 9 mg min⁻¹:
(a) tilt 0°, (b) tilt +45°.

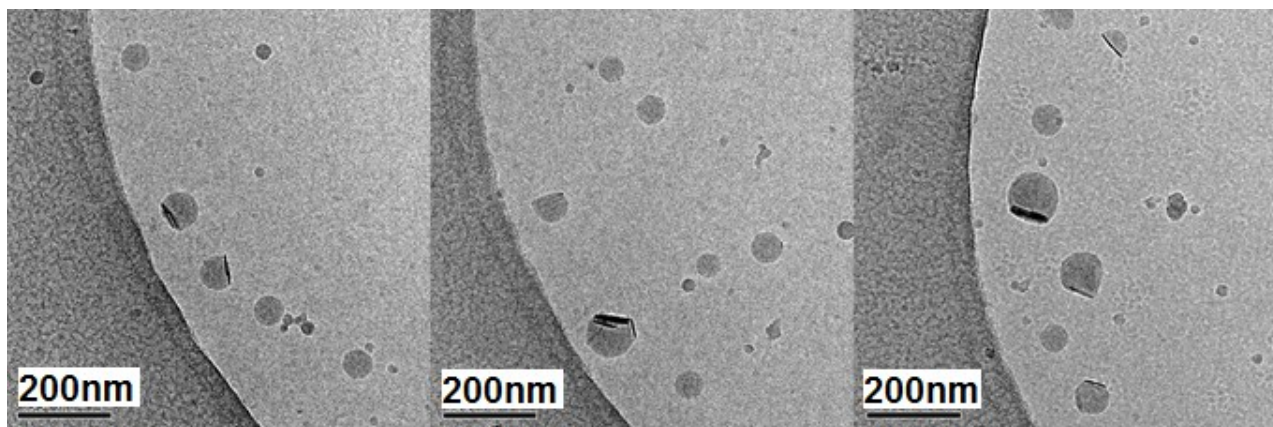


Figure S6. cryo-TEM images of polymer-Gibbsite latex particles obtained at the feed rate = 18 mg min^{-1} .

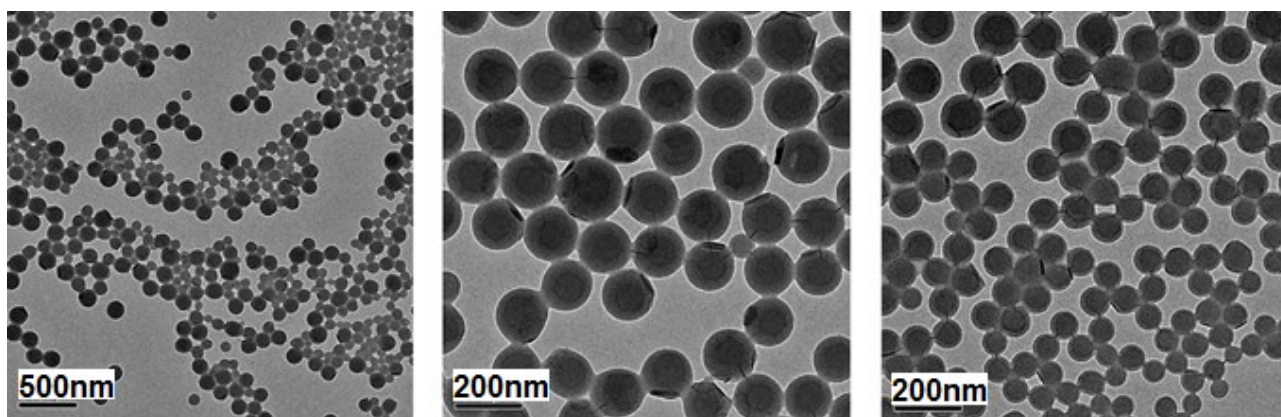


Figure S7. TEM images of polymer-Gibbsite latex particles obtained at the feed rate = 90 mg min^{-1} .

Potential loss of Br endgroups during hydrolysis of *t*-BA groups

The initiator ethyl α -bromoisobutyrate was subjected to the same hydrolysis conditions as the BA-*co-t*BA cooligomers and was characterized before and after reaction by ^1H and ^{13}C NMR. The spectra shown in Figure S8 show that there is no significant loss in Br functionality.

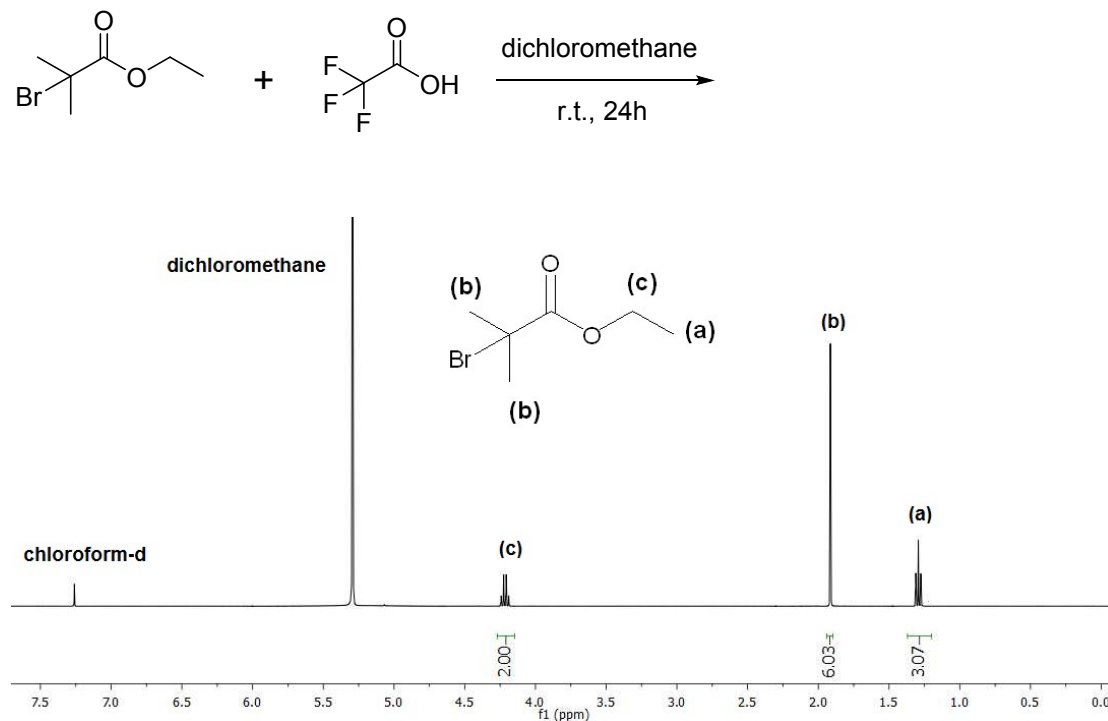


Figure S8a. ^1H NMR (CDCl₃) of ethyl α -bromoisobutyrate in dichloromethane: $\delta(\text{CH}_3)=1.29$, $\delta(\text{C}-(\text{CH}_3)_2)=1.92$, $\delta(\text{O}-\text{CH}_2)=4.25$.

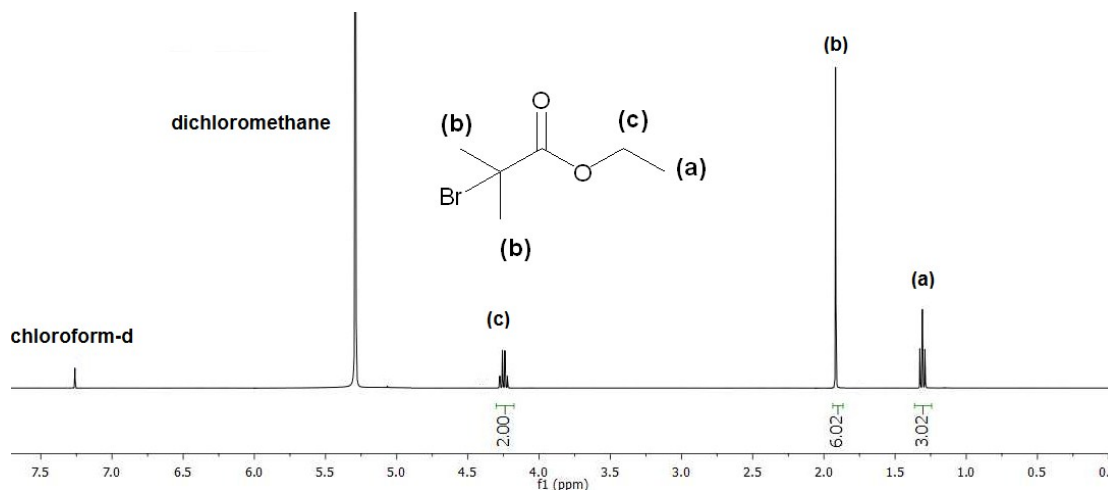


Figure S8b. ^1H NMR (CDCl₃) of ethyl α -bromoisobutyrate in dichloromethane after addition of TFA (24h): $\delta(\text{CH}_3)=1.3$, $\delta(\text{C}-(\text{CH}_3)_2)=1.91$, $\delta(\text{O}-\text{CH}_2)=4.23$.

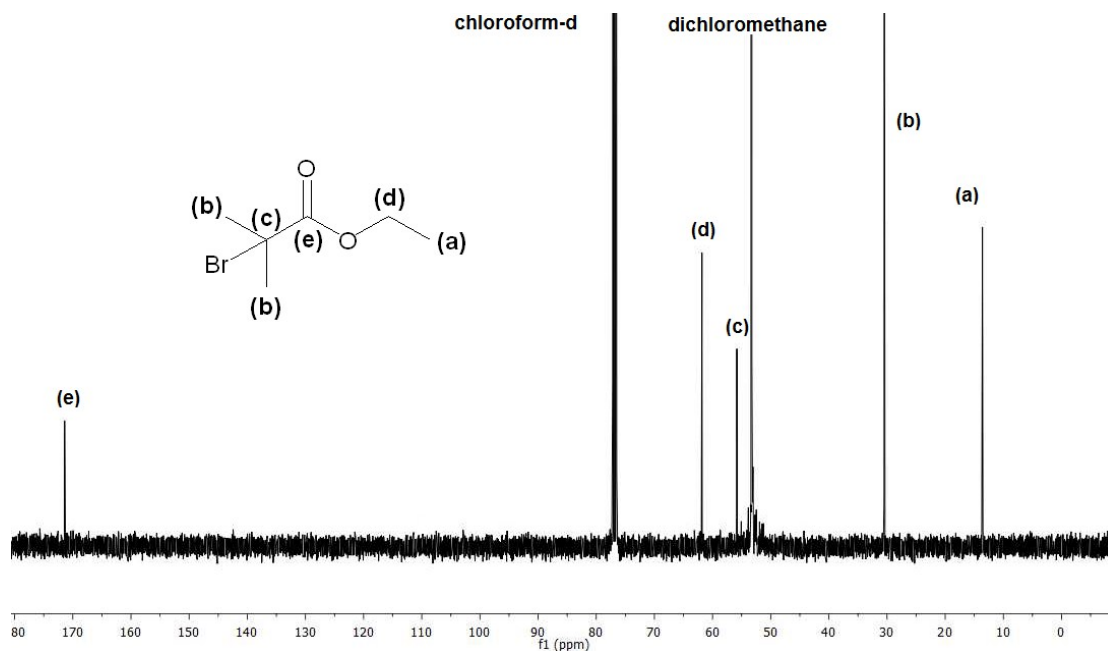


Figure S8c. ^{13}C NMR (CDCl_3) of ethyl α -bromoisobutyrate in dichloromethane: $\delta(\text{CH}_3)=13.60$, $\delta(\text{C}-(\text{CH}_3)_2)=30.50$, $\delta(\text{Br}-\text{C}-(\text{CH}_3)_2)=55.82$, $\delta(\text{O}-\text{CH}_2)=61.82$, $\delta(\text{C}=\text{O})=171.41$.

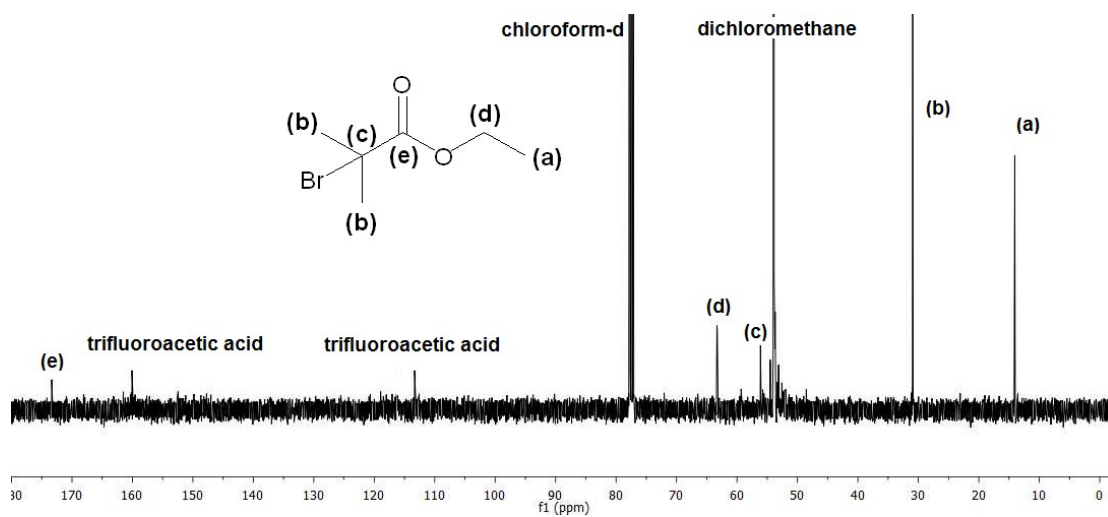


Figure 8d. ^{13}C NMR (CDCl_3) of ethyl α -bromoisobutyrate in dichloromethane: $\delta(\text{CH}_3)=14.01$, $\delta(\text{C}-(\text{CH}_3)_2)=30.95$, $\delta(\text{Br}-\text{C}-(\text{CH}_3)_2)=56.01$, $\delta(\text{O}-\text{CH}_2)=62.01$, $\delta(\text{C}=\text{O})=171.98$. Trifluoroacetic acid: $\delta(\text{COOH})=113.33$, $\delta(\text{C}-\text{F}_3)=161.24$